Estimation of Branch Angle from 3D Point Cloud of Plants

Lu Lou[1,3], Yonghuai Liu[1], Minglan Shen[3], Jiwan Han[2], Fiona Corke[2] and John H. Doonan[2]

[1]Department of Computer Science, Aberystwyth University,United Kingdom, SY23 3DB,
[2]National Plant Phenomics Centre, IBERS, Aberystwyth University, United Kingdom, SY23 3DB
[3]College of Information Science and Engineering, Chongqing Jiaotong University, China, 400074
lul1@aber.ac.uk, yyl@aber.ac.uk

Abstract

Measuring geometric features in plant specimens either quantitatively or qualitatively, is crucial for plant phenotyping. However, traditional measurement methods tend to be manual and can be tedious, or employ coarse 2D imaging techniques. Emerging 3D imaging technologies show much promise in capturing architectural complexity. However, automated 3D acquisition and accurate estimation of plant morphology for the construction of quantitative plant models remain largely aspiration. In this paper, we propose an approach for segmentation and angle estimation directly from dense 3D plant point clouds. Experimental results show that the approach is efficient and reliable, and appears to be a promising 3D acquisition and measurement solution to plant phenotyping for structural analysis and for building Functional-Structural Plant Models (FSPM).

1. Introduction

Functional-structural plant models (FSPM) seek to integrate geometric structure with function, i.e. the flow of material and energy through a system as dependent on the genotype and as modified by environmental influences. FSPMs attempt to simulate growth and development through modelling the development, growth and function of individual cells, tissues, organs and plants in their spatial and temporal contexts. Accurate models are often associated with 3D visualization of the plant architecture and FSPMs (or virtual plants) attempt to explicitly describe development over time [21] [28] [33] [32]. Early the most influential work, Lindenmayer-Systems (commonly named L-Systems), was done by Lindenmayer [13] and Prusinkiewicz et al. [21]. L-Systems are a formal language developed to describe both static plant structure and its dynamics (driven by functions) in the form of a set of intuitive rules. The central idea of L-systems consists of rewriting of a string of modules representing the structure of the plant. Explicit rewriting rules express the creation and changes of state of the modules over time. Such rules can be expressed using a dedicated programming language ([22]) or by incorporating L-system based language constructs into existing languages, such as C++ (L+C) [10] , Java (GroIMP) [11]) or Python (L-Py and GreenLab) [1].

According to the formalism of L-systems, a plant is viewed as a developing assembly of individual units, or modules. These modules are characterized by parameters such as length, width, and age, as well as parameters characterizing shape. A methodology for constructing L-system models based on empirical estimates of such parameters has been introduced by [23]. Many papers describe the use of different types of equipment (e.g. rulers, protractors, sonic or magnetic digitizers) to collect data on the spatial orientation and shape of organs and how to process such data to arrive at mathematical descriptions of shapes and angles and, finally, at the reconstruction of a simulated plant structure in silico [29] [7] [8] [6] [4] [36]. An empirical model of Arabidopsis was presented in [17], which simulates and realistically visualizes development of aerial parts of the plant from seedling to maturity. This model integrates thousands of measurements data including sizes and shapes of individual organs (internodes, leaves, and flower organs, etc.), taken from several plants at frequent time intervals destructively and non-destructively. A comparison of selected developmental stages of an individual plant over time was made in [17] (Fig. 1). The comparison indicates that the model captures the architecture of a growing Arabidopsis plant faithfully, but there is obviously difference between 3D models and real plants, because the values of measured parameters are averaged over several plants, as well as some empirical parameters in L-systems lack explicit physical meanings [17].

Plant phenotyping underpins much of plant biology and breeding, and involves the routine measurement of characteristics or traits. Traditionally, phenotyping has been of-

978-1-4673-8332-5/15 $31.00 © 2015 IEEE
DOI 10.1109/3DV.2015.68

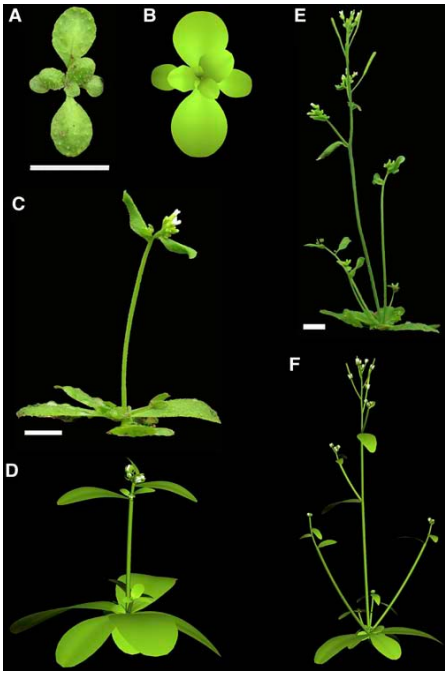

Figure 1. Comparison of sample Arabidopsis plants (A, C, E) with the model (B, D, F) after different hours from seeding (HFS). A and B, at 264 HFS; C and D, at 417 HFS; E and F, at 491 HFS. Scale bar =1cm. The figure is taken from [17].

ten destructive but the dynamic objective measurement of traits as they change in response to genetic mutation or environmental influences is an important goal that could provide additional insight into the underlying processes that control development. The phenotype of an individual organism emerges from the interaction of its genotype with its developmental history and immediate environment. The range of phenotypes therefore can be large, even for a single genotype. In recent years, various high-throughput plant growth and phenotyping platforms have been developed, for example, PHENOPSIS [9] is used by French National Institute for Agricultural Research (INRA) for Arabidopsis. TraitMillTM [25] is developed by the company CropDesign and used for evaluation of transgenic rice (Oryza sativa). Commercial high-throughput phenotyping platforms [12] based on automated plant handling and imaging systems have been installed at Australian Centre for Plant Genomics (ACPFG), the Leibniz Institute of Genetics and Crop Plant Research (IPK) in Gatersleben, and The National Plant Phenomics Centre (NPPC) of IBERS of Aberystwyth University in the UK. In such systems, morphological and physiological data are captured by a variety of sensors [12]: RGB camera, infrared camera, and near infrared camera, etc. These high-throughput plant phenotyping platforms are aimed at reducing manual acquisition of phenotypic data.

The ability to capture accurate 3D information from a growing plant efficiently at any given time is attractive for both FSPM and plant phenotyping. Such models can contain the information needed to compute a variety of plant traits, such as total leaf shape and area, branch angle, etc., and are essential where other data (fluorescence, thermal etc) needs to be co-registered with the complex surface morphology of the plant. Therefore, there is an urgent need for rapid, automated, and generalized techniques for accurately reconstructing and measuring the 3D architecture of complex plants.

Our goal aims at developing suitable measurement techniques towards diverse plants (in view of the variety and complexity of observing plant architecture). In the following, we briefly describe the framework of 3D data acquisition based on multi-view images and pre-processing of 3D point clouds in Section 2. In Sections 3 and 4, we propose a segmentation method using spectral clustering and an approach for estimating the angles of segmented branches respectively. Finally, we show the experimental results in Section 5 and conclude the paper in Section 6.

2. Methods

2.1. Acquisition of 3D Data of plants

Recently, several methods have been developed to capture the 3D structure of entire plants non-destructively and then build accurate models for visualization, measurement and analysis. These methods include laser scanning, digital camera photography, and structured light range scanning.

We compared several existing methods of 3D reconstruction and concluded that the 3D LASER/LIDAR scanner or the structured-light scanner (including Kinect sensor) do not work well on plants, especially on complex or even marginally occluded specimens or on small plants. This conclusion is consistent with that proposed in [16]. Therefore, inspired by [15], we have built an efficient and accurate multiview image-based 3D reconstruction system that could cope with a diversity of plant form and size, while using equipment available in most biology labs. Briefly, the system can be divided into three main modules: structure from motion, stereo matching and depth map merging. The algorithm details are referred to read existing work in [15]. Fig. 2 illustrates the framework.

We used a single camera (Canon 600D with *18-55mm* variable focus lens) and a turn-table to capture tens of thousands of plant images (3696×2448 high-resolution) without calibration required in advance, and built up a dataset of 3D plant point cloud of various plants (including *Arabidopsis thaliana*, oat, wheat, maize, foragegrass (*lolium*), clover, physalis, brassica, etc.).

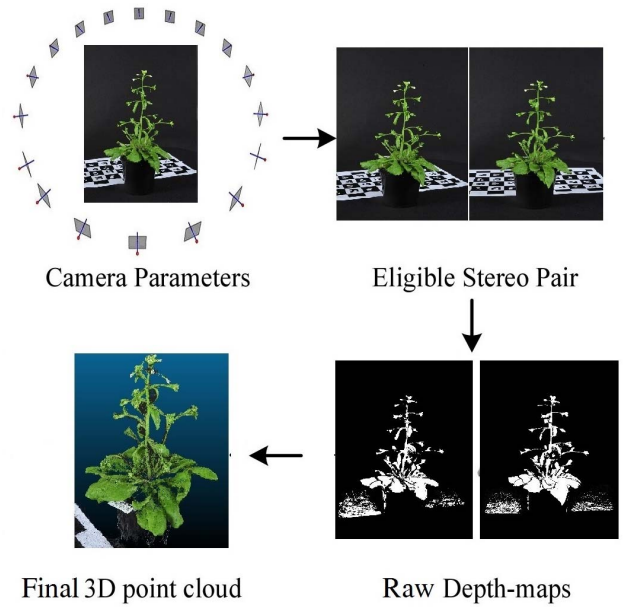

Figure 2. 3D reconstruction framework

2.2. Pre-processing for the raw 3D points

After 3D acquisition of plants, we obtained the dense 3D point clouds. These points are corrupted by imaging noise, registration error, and outliers. There are a large number of redundant points. A 3D plant is usually represented by millions of points with color information. We have to pre-process the data, such as noise removing, down-sampling, etc., before further analysis.

Noise removing. Because we captured the multiview images of plants in controlled environment, the colors of most of 3D noisy points in the raw dataset are close to black (we used a black curtain as background) and can be clearly distinguished from those 3D organ points whose colors are almost green. Therefore, we adopted a color filter to remove the 3D noisy points effectively.

Down-sampling. In our work, while such a large number of points are useful to describe the details of a plant of interest, it is time consuming to process and analyze such data. To reduce the computational complexity, a sampling method was used to down-sample the raw 3D point cloud to a sparse point cloud with less than twenty thousand points. Considering that 3D point cloud are incomplete (mainly caused by occlusion) and densities are not even, we employed "Merge Close Vertices" filter in Meshlab. This filter merges the close neighboring points together if their distances are smaller than the specified distance threshold. The threshold used in our work is not fixed value, depending on different plants, it can be adjusted from 0.005% to 0.05% of the diagonal length of the enclosing box that surrounds the 3D points.

Normal estimation. The normal of each sampled point was estimated using the method proposed in [30] where the number of neighbours was set as $K = 30$ for accuracy and stability.

3. Segmentation of 3D Points of Plants

The problem of segmenting and skeletonizing plant structure in 3D point clouds remains challenging due to many reasons: occlusion, imaging noise, thin and pseudo-linear structure, and closeness of one part to another. Previous work usually focused on scenes (outdoor/indoor), buildings, man-made objects like toy, desk, chair, car, or CAD models. Most of them have abundant characteristics, such as flat surfaces, colors, textures, well-defined geometric sizes or shapes (plane, cylinder, sphere, etc.), which are helpful for segmentation of a single object. Many algorithms have been proposed to decompose an object into functionally meaningful parts or regions, including region growing, K-means, hierarchical clustering and spectral clustering [14] [27] [26]. For segmentation of 3D point clouds of plant material, most work focused on detecting different organs using features training and classfication, or by means of known information like leaf size, stem size, colors, etc. These methods were only applicable to limited plants [19] [5] [20].

We employed spectral clustering to segment the sampled points in this paper.

Spectral Clustering [31] is described by an undirected complete similarity graph $G = (V, E)$ where V is a set of vertices v_i with one vertex for each of n points in the original data and E is an edge set of similarities $s_{ij} = s_{ji}$ between pairs of points. The s_{ij} is defined by user to denote local neighborhood relations between data points, such as distance, etc.. If s_{ij} is larger than a certain threshold, two vertices are connected and the edge is weighted by s_{ij}. The weighted adjacency matrix $\mathbf{W}$ is the $n \times n$ symmetric matrix of pair-wise similarities between points as defined:

$$\mathbf{W} := (w_{ij})_{i,j=1,...,n} \geq 0 \tag{1}$$

The degree of a vertex $v_i \in \mathbf{V}$ is defined as

$$d_i := \sum_{j=1}^{n} w_{ij} \tag{2}$$

Degree matrix $\mathbf{D}$ is defined as the diagonal matrix with $d_1, ..., d_n$ on the main diagonal.

The degree matrix $\mathbf{D}$ summarizes the similarity of each vertex with respect to the other vertices as a whole, whereas the similarity matrix $\mathbf{W}$ summarizes pair-wise similarities between vertices. To compute spectral features, G is expressed as an $n \times n$ Laplacian matrix. There are a number of definitions for the Laplacian [31], we use the simplest

one, $\mathbf{L} = \mathbf{D} - \mathbf{W}$, where the matrix $\mathbf{L}$ is symmetric, positive semi-definite with smallest eigenvalue equal to 0. To construct spectral features, the eigenvectors associated with the k largest eigenvalues of $\mathbf{L}$, are formed into an $n \times k$ matrix $\mathbf{F}$. Spectral features associated with the i^{th} vertex, are taken from the i^{th} row of $\mathbf{F}$.

Generally speaking, all the spectral clustering algorithms applied in [26] [14] are intrinsically similar, and the main differences are in creating the similarity matrix and in how to select the parameters such as thresholds and the number of clusters. Our method differs from previous work [14] which focus on 3D mesh segmentation for CAD models: (i) Considering shape complexity, sufficient 3D points are needed to represent a plant in our dataset where there are $10K-50K$ down-sampling points, more than usually a few thousand points in 3D CAD models; (ii) We constructed an undirected K-nearest neighbor similarity graph by connecting vertex v_i with vertex v_j if v_j is among the K-nearest neighbors of v_i and weighting the edge with 1, if the including angle between their normals is smaller than 1°; 0 otherwise; (iii) We Computed the unnormalized Laplacian L, L=D-W; (iv) We then employed a standard spectral clustering method to cluster points into initial segments, where the number K (K=75) of clusters was selected empirically to get initial results with over-segmentation; (v) We finally combined neighboring segments according to their normal similarity (threshold 10°) to produce the final segmentation results. The proposed method is summarized in Algorithm 1.

Algorithm 1 The segmentation of a 3D point cloud

Input: point cloud $V = \{v_i \in \mathbb{R}^3, 1 \leq i \leq n\}$.

1: Down-sampling 3D point cloud V.
2: Construct a similarity graph G.
3: Compute the unnormalized Laplacian L.
4: Perform spectral clustering on L.
5: Combine the neighboring clusters with similar normals.

Output: A segmented point cloud.

4. Estimation of Angles of Branches

The angle of two branches is defined as the angle included by two axes of two branches, where two branches are approximated as two mini-bounding boxes. Branch angles are very important parameters that directly determine the structure of a plant in an L-system-based model. Usually, the angle was supposed as initial constant empirical value with a fixed changing rate. The branch angle of a real plant is also affected by environmental factors. To measure the angles of branches directly from a 3D point cloud is very attractive.

4.1. Skeleton of 3D plant points

We firstly made an effort to compute the branches' angle through abstracting the skeleton of 3D plant points. Unlike some man-made objects, where the skeletons of objects are sometimes ambiguous or even meaningless, the skeleton of a 3D plant point cloud can clearly represent the structure of the plant. But extraction of the skeleton of a leaf is a challenging problem because of its variable contour and intrinsic thinness. However, for L-systems, it is only necessary to define the contour of a leaf and not its skeleton. Therefore, when leaves are segmented, we manually remove them from the point cloud and then adopt a skeletonisation process to extract the basic branch-structure of the plant. Due to occlusion the plant point cloud is normally incomplete, and the density of points varies from one region to another. In order to extract a skeleton with accurate and complete connectivity, the topological thinning method proposed by Cao [3] was adopted. This method is based on Laplacian contraction, and it has the clear advantage that not only is it robust to noise but it also produces a well connected skeleton.

Nevertheless, we had found that the skeletons of two neighboring branches cannot always accurately represent the medial axis (a case shown in Fig. 6) so that it is too difficult to calculate the angle as we expected.

4.2. Estimation of angles of branches using bounding boxes

3D Bounding boxes are three-dimensional boxes (eight corners) that surround entities within the measuring model. The mini-3D bounding box is such a box that has a minimum volume, and was proven that at least its two adjacent box sides are flush with edges of the hull [18]. For simplisity, a 2D bounding box is illustrated in Fig. 3, where a min bounding rectangle can be found by means of rotating the convex hull and calculating the minimum rectangle area.

It is a basic assumption in our proposed segmentation method that the 3D mini-bounding box surrounding a branch has a longest edge that parallels the axis of the branch. Therefore, we firstly employed 3D mini-bounding box algorithm to obtain the mini 3D bounding box corresponding to each segmented "branch" (chose manually because organ classfication hasn't been implemented in this paper), and then calculate including angle of two longest edges of the two mini-bounding boxes (as shown in Fig. 7). We supposed this including angle could approximate the angle of two branches (see Fig. 8). The method is described in Algorithm 2.

5. Experimental Results and Analysis

The experiments were performed on an Intel Core i7 2.7GHz machine with 16GB RAM. In the experiment of

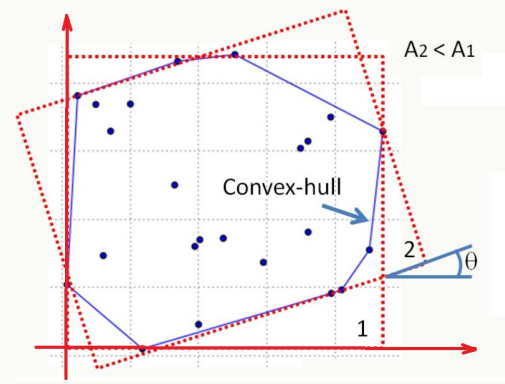

Figure 3. 2D mini-bounding box

Algorithm 2 Branch angle estimation

Input: Segmented point cloud V.

1: Manually identify those segments of interest that can represent the branches.
2: Compute the convex hull of two selected segments ("branches") respectively.
3: Find out two 3D bounding boxes of the two branches with minimum volumes
4: Find out the longest edges of two mini 3D bounding boxes

Output: The including angle of the longest edges.

spectral clustering segmentation, the majority of the computational time was actually spent on constructing the similarity matrix, which depended on the number of 3D points, but was typically around 6 minutes for $20K$ points. Comparatively, the clustering time was almost negligible. The segmentation results of selected plants are shown in Fig. 4.

We had also compared the proposed segmentation method with the standard K-means algorithm. From the results in Fig. 4, we can see that obviously the K-means just cluster the points in proportional spacing without considering the local connectivities, and the proposed method excelled the K-means in each selected plant. Furthermore, the K-means algorithm requires a choice of the number K of clusters, but this is certainly a difficult issue especially for complex datasets like plants. Quantitative evaluation of the segmentation quality is difficult because either the the ground truth is missing, or the effectiveness of the segmentation is determined by the application for which it is intended. However, we found that: i) Our approach is applicable to diverse plant species – only use raw 3D point data as the input not considering the other information such as shape, color, size, etc.; ii) Satisfactory segmentation on 3D points of plants with various shapes is really a rather difficult problem – it is not always possible to get meaningful and accurate segmentation, especially for leaves with

(a) Arabidopsis rosette (3 weeks growing, 60 images); 148857 3D points; 12111 3D points, K=10 in K-means.

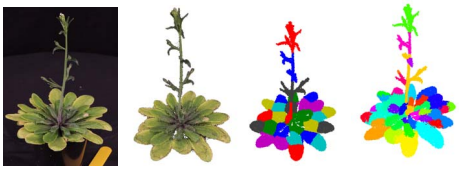

(b) flowering Arabidopsis (6 weeks growing, 60 images); 712540 3D points; 19007 3D points, K=30 in K-means.

(c) physalis (90 images); 322020 3D points; 9591 3D points, K=10 in K-means.

(d) maize (120 images) ; 906012 3D points; 8882 3D points, K=20 in K-means.

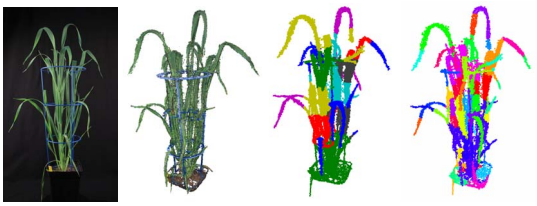

(e) wheat (120 images) ; 2128586 3D points; 11792 3D points, K=20 in K-means.

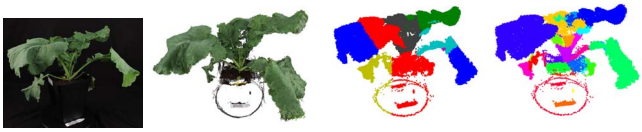

(f) brassica (120 images) ; 1588773 3D points; 28319 3D points, K=10 in K-means.

Figure 4. 3D segmentation of various plants. 1st column: one of 2D images. 2nd column: 3D points after down-sampling. 3rd column: segmentation using standard K-means. 4th column: segmentation using the proposed method.

curved surfaces, or tiny side-branches at the top of an *Arabidopsis* flowering stem, and at most junction points of a plant.

The skeletonization result of a sample plant is illustrated in Fig. 5(d). It can be seen that the skeleton produced is representative of the plant structure. Although the skeleton cannot be used to estimate the angle of branches in this work, the plant skeleton cloud be potentially parsed to syntax expression to define the architecture rules of L-systems in our further research.

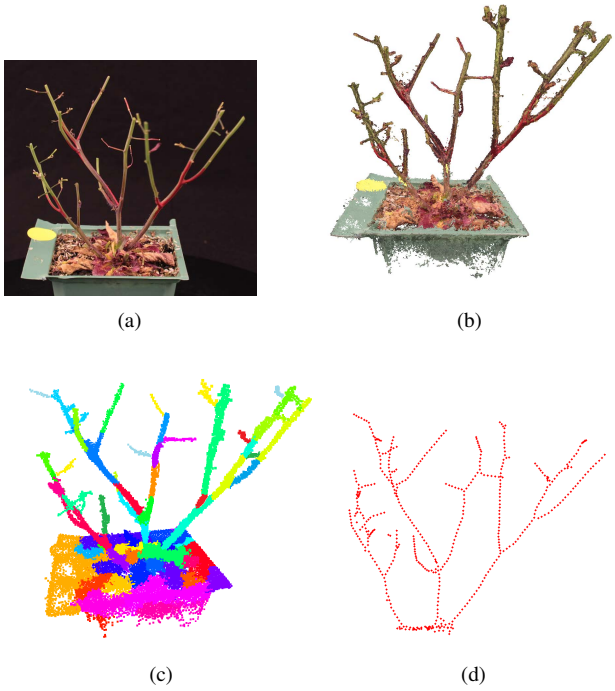

(a) (b) (c) (d)

Figure 5. (a) Raw 2D image of an Arabidopsis (leaves cut off) (b) 3D point cloud. (c) segmented 3D points. (d) 3D skeleton points.

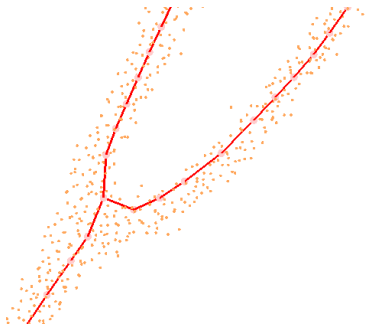

Figure 6. The skeleton of two branches

We used the plant model in Fig. 5(b) to obtain a set of measured angles, then compared those with the values obtained by manual measurement by a biologist. The measurement results of a number of branch angles are shown in Table. 1, and the root mean square error (RMSE) of the estimated angles is 1.88°.

To the best of our knowledge, there does not exist any method in the literature for angle estimation from 3D plant point clouds. Thus we used a protractor as a measuring reference and produced a set of its 3D point clouds with different angles varied from 20°to 90°, and then calculated the angles of its bars using the proposed method in Section 4 (shown in Fig. 9). The results are shown in Table. 2, and the root mean square error (RMSE) of the estimated angles is 0.45°. These results show that our proposed method is reliable. Nevertheless, it should be noted that this method is dependent on the segmented branches, since segmented branches are identified and chosen manually.

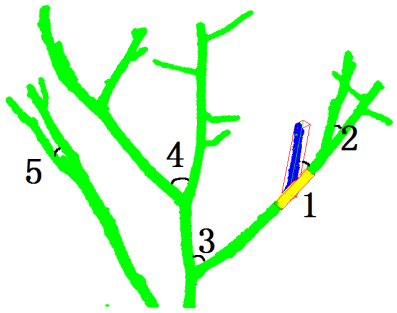

Figure 7. The angle included by two mini-bounding boxes

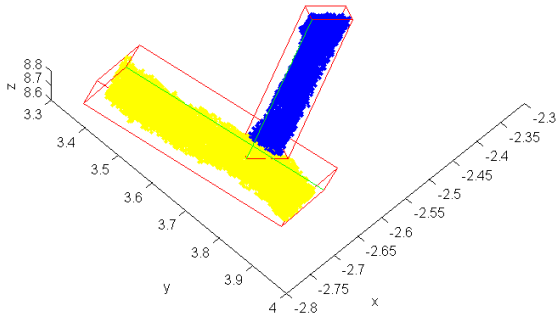

Figure 8. Two mini-bounding boxes are used to approximate two branches

6. Conclusion

This paper has proposed a novel automatic 3D point cloud segmentation method through adapting the spectral clustering algorithm, which is applicable to diverse plants with varied structure, size and shape, and then has proposed an interactive approach for estimation of angles between branches obtained from the aforementioned segmentation

Item	Ground truth	Estimated value	Error(%)
angle1	59.80	58.70	-1.89%
angle2	52.40	49.40	-5.73%
angle3	61.90	63.30	2.26%
angle4	69.20	68.57	-0.91%
angle5	39.80	42.06	5.68%
Error (RMSE)		1.88	

Table 1. Errors of estimated angles (in degrees)

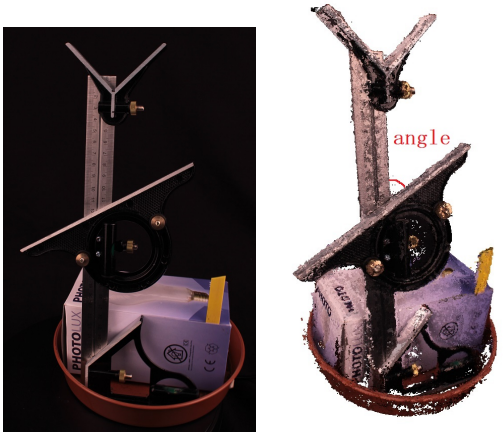

(a) (b)

Figure 9. (a) A raw 2D image of an protractor (b) A 3D point cloud of the protractor.

Item	Ground truth	Estimated value	Error(%)
angle-20°	20	19.47	-2.64%
angle-22°	22	22.33	1.52%
angle-30°	30	30.45	1.50%
angle-38°	38	38.34	0.88%
angle-45°	45	44.33	-1.48%
angle-50°	50	50.42	0.85%
angle-60°	60	60.24	0.39%
angle-70°	70	70.56	0.79%
angle-90°	90	89.65	-0.38%
Error (RMSE)		0.45	

Table 2. Errors of estimated angles (in degrees)

step. Our contribution can be summarised into two aspects: (i) we expanded existing computer vision techniques for the new tasks operating -successfully- on spatially complicated plant data, (ii) through the experiments, we revealed the limitations of the existing techniques.

For the proposed segmentation method, the main limitation is that component recognition could be further refined −for example, the leaves sometimes contain aspects of petiole or stem, depending on plant morphology and architectural complexity. Fully automated 3D segmentation that can cope with a wide range of different shaped plants is still a rather challenging problem, because segmentation is often determined by points and a meaningful segmentation on a plant can be quite different in other plant species or morphological mutants. An efficient segmentation method may require a combination of machine learning [34], prior knowledge [35][2], or user intervention [24].

The angle estimation method is relatively easier compared with analyzing the parameters of other organs, but its quality depends on the results of segmentation and each segmented branch has also to be chosen manually. Manual and destructive methods remain the sole cost-effective method open to most biologists but fully automated methods are indeed the ultimate goal of computer vision efforts in plant phenotyping. The development of completely automatic algorithms is beyond the scope of our current project and will require substantially more resources to realise this ambitious goal. In future work, we will focus on developing automatic segmentation/classification methods to measure various organs of plants, and improving analysis ability of plant phenotyping.

Acknowledgements

We acknowledge funding from the European Union FP7 Capacities Programme (Grant Agreement No. 284443: European Plant Phenotyping Network, an Integrating Activity Research Infrastructure project) and BBSRC NCG Grant Ref: BB/J004464/1. We would like to thank the members of the NPPC of IBERS of Aberystwyth University for providing plant material and help on image acquisition.

References

[1] F. Boudon, C. Pradal, T. Cokelaer, P. Prusinkiewicz, and C. Godin. L-py: an L-system simulation framework for modeling plant architecture development based on a dynamic language. *Frontiers in Plant Science*, 3, 2012. 1

[2] D. Bradley, D. Nowrouzezahrai, and P. Beardsley. Image-based reconstruction and synthesis of dense foliage. *ACM Transactions on Graphics (TOG)*, 32(4):74, 2013. 7

[3] J. Cao, A. Tagliasacchi, M. Olson, H. Zhang, and Z. Su. Point cloud skeletons via laplacian based contraction. In *International Conference on Shape Modeling, 2010*, pages 187–197. IEEE, 2010. 4

[4] J. Dauzat, P. Clouvel, D. Luquet, and P. Martin. Using virtual plants to analyse the light-foraging efficiency of a low-density cotton crop. *Annals of Botany*, 101(8):1153–1166, 2008. 1

[5] D. Dey, L. Mummert, and R. Sukthankar. Classification of plant structures from uncalibrated image sequences. In *IEEE Workshop on Applications of Computer Vision (WACV)*, pages 329–336. IEEE, 2012. 3

[6] T. Dornbusch, P. Wernecke, and W. Diepenbrock. A method to extract morphological traits of plant organs from 3d point clouds as a database for an architectural plant model. *Ecological Modelling*, 200(1):119–129, 2007. 1

[7] J. Drouet. Modica and modanca: modelling the three-dimensional shoot structure of graminaceous crops from two methods of plant description. *Field Crops Research*, 83(2):215–222, 2003. 1

[8] J. B. Evers, J. Vos, C. Fournier, B. Andrieu, M. Chelle, and P. C. Struik. Towards a generic architectural model of tillering in gramineae, as exemplified by spring wheat (triticum aestivum). *New Phytologist*, 166(3):801–812, 2005. 1

[9] C. Granier and et al. Phenopsis, an automated platform for reproducible phenotyping of plant responses to soil water deficit in arabidopsis thaliana permitted the identification of an accession with low sensitivity to soil water deficit. *The New Phytologist*, 169:623–635, 2006. 2

[10] R. Karwowski and P. Prusinkiewicz. Design and implementation of the l+ c modeling language. *Electronic Notes in Theoretical Computer Science*, 86(2):134–152, 2003. 1

[11] O. Kniemeyer and W. Kurth. The modelling platform groimp and the programming language xl. In *Applications of Graph Transformations with Industrial Relevance*, pages 570–572. Springer, 2008. 1

[12] LemnaTec. Image process in biology. 2

[13] A. Lindenmayer. Mathematical models for cellular interactions in development i. filaments with one-sided inputs. *Journal of Theoretical Biology*, 18(3):280–299, 1968. 1

[14] R. Liu and H. Zhang. Segmentation of 3d meshes through spectral clustering. In *Proceedings of 12th Pacific Conference on Computer Graphics and Applications*, pages 298–305, 2004. 3, 4

[15] L. Lou, Y. Liu, J. Han, and J. H. Doonan. Accurate multi-view stereo 3d reconstruction for cost-effective plant phenotyping. In *Proceedings of the Int. Conf. on Image Analysis and Recognition*, pages 349–356. Springer, 2014. 2

[16] L. Lou, Y. Liu, M. Sheng, J. Han, and J. H. Doonan. A cost-effective automatic 3d reconstruction pipeline for plants using multi-view images. In *Proceedings of the Int. Conf. on TAROS 2014*, pages 221–230. Springer, 2014. 2

[17] L. Mündermann, Y. Erasmus, B. Lane, E. Coen, and P. Prusinkiewicz. Quantitative modeling of arabidopsis development. *Plant Physiology*, 139(2):960–968, 2005. 1, 2

[18] J. O'Rourke. Finding minimal enclosing boxes. *International Journal of Computer & Information Sciences*, 14(3):183–199, 1985. 4

[19] S. Paulus, J. Dupuis, A.-K. Mahlein, and H. Kuhlmann. Surface feature based classification of plant organs from 3d laserscanned point clouds for plant phenotyping. *BMC Bioinformatics*, 14(1):238, 2013. 3

[20] S. Paulus, J. Dupuis, S. Riedel, and H. Kuhlmann. Automated analysis of barley organs using 3d laser scanning: An approach for high throughput phenotyping. *Sensors*, 14(7):12670–12686, 2014. 3

[21] P. Prusinkiewicz and J. Hanan. Visualization of botanical structures and processes using parametric l-systems. In *Scientific visualization and graphics simulation*, pages 183–201. John Wiley & Sons, Inc., 1990. 1

[22] P. Prusinkiewicz, J. Hanan, and R. Měch. An l-system-based plant modeling language. In *Applications of graph transformations with industrial relevance*, pages 395–410. Springer, 2000. 1

[23] P. Prusinkiewicz, W. Remphrey, C. Davidson, and M. Hammel. Modeling the architecture of expanding fraxinus pennsylvanica shoots using l-systems. *Canadian Journal of Botany*, 72(5):701–714, 1994. 1

[24] L. Quan, P. Tan, G. Zeng, L. Yuan, J. D. Wang, and S. B. Kang. Image-based plant modeling. *ACM Transactions on Graphics (TOG)*, 25:599–604, 2006. 7

[25] C. Reuzeau. Traitmill (TM): A high throughput functional genomics platform for the phenotypic analysis of cereals. *In Vitro Cellular & Developmental Biology-Animal*, 43:S4–S4, 2007. 2

[26] A. Shamir. Segmentation and shape extraction of 3d boundary meshes. *State-of-the-Art Report, Proceedings Eurographics*, 2006:137–49, 2006. 3, 4

[27] S. Shlafman, A. Tal, and S. Katz. Metamorphosis of polyhedral surfaces using decomposition. In *Computer Graphics Forum*, volume 21, pages 219–228, 2002. 3

[28] R. Sievänen and et al. Components of functional-structural tree models. *Annals of Forest Science*, 57(5):399–412, 2000. 1

[29] H. Sinoquet, P. Rivet, C. Godin, et al. Assessment of the three-dimensional architecture of walnut trees using digitising. *Silva Fennica*, 31:265–273, 1997. 1

[30] G. Taubin. Estimating the tensor of curvature of a surface from a polyhedral approximation. In *Proc. ICCV*, pages 902–907. IEEE, 1995. 3

[31] U. Von Luxburg. A tutorial on spectral clustering. *Statistics and Computing*, 17(4):395–416, 2007. 3

[32] J. Vos and et al. Functional–structural plant modelling: a new versatile tool in crop science. *Journal of Experimental Botany*, 61(8):2101–15, 2009. 1

[33] J. Vos, L. Marcelis, and J. Evers. Functional-structural plant modelling in crop production: adding a dimension. *Frontis*, 22:1–12, 2007. 1

[34] K. Yamamoto, W. Guo, Y. Yoshioka, and S. Ninomiya. On plant detection of intact tomato fruits using image analysis and machine learning methods. *Sensors*, 14(7):12191–12206, 2014. 7

[35] C. Zhang, M. Ye, B. Fu, and R. Yang. Data-driven flower petal modeling with botany priors. In *IEEE Conference on Computer Vision and Pattern Recognition*, pages 636–643, 2014. 7

[36] B. Zheng, L. Shi, Y. Ma, Q. Deng, B. Li, and Y. Guo. Comparison of architecture among different cultivars of hybrid rice using a spatial light model based on 3-d digitising. *Functional Plant Biology*, 35(10):900–910, 2008. 1